Received August 24, 2019, accepted September 5, 2019, date of publication September 10, 2019,
date of current version September 25, 2019.

Digital Object Identifier 10.1109/ACCESS.2019.2940616

A Novel Wideband Low-RCS Reflector by Hexagon Polarization Rotation Surfaces

ZHOU-HU DENG[1,2], FU-WEI WANG[1,2], YU-HUI REN[1], (Member, IEEE), KE LI[1], (Member, IEEE), AND BAO-JIAN GAO[1]

[1]School of Information Technology, Northwest University, Xi'an 710127, China
[2]The Radio Communication Association of Xi'an, Xi'an 710075, China

Corresponding authors: Fu-Wei Wang (wfw@nwu.edu.cn) and Bao-Jain Gao (405686893@qq.com).

This work was supported in part by the Natural Science Basic Research Plan in Shaanxi Province of China under Grant 2018JQ6102 and Grant 2018JM6077, in part by the International Cooperation Foundation of Shaanxi Province, China, under Grant 2018KW-024, in part by the Key Academic Communication and Technology service project of Xi'an Association for Science and Technology under Grant 201854, and in part by the Young Talent Fund of Xi'an Association for Science and Technology under Grant 201709.

ABSTRACT In this paper, a novel wideband Low-Radar Cross Section (RCS) reflector is proposed. It consists of metallic hexagonal patches on the top layer of dielectric substrate and a metallic film on the bottom. The patches are consists of different sizes of hexagonal patch arrays. They are corresponding to different resonance frequencies, respectively. And the wideband polarization rotation is achieved. A 180°-phase difference is created by the Polarization Rotation Surfaces (PRS) using chessboard-like geometry, which introduced 90° and −90° phase-shift, respectively. The scattering energy is redirected into off-normal directions by the PRS, which enables the effective RCS reduction. In order to obtain more RCS reduction, the arrangement of the PRS reflector has been optimized. The results show that, more RCS reduction can be achieved by the improved arrangement. The monostatic RCS of the reflector can be reduced more than 20 dB by this method.

INDEX TERMS Polarization rotation surfaces (PRS), radar cross section (RCS) reduction, hexagonal.

I. INTRODUCTION

Radar cross section (RCS) is defined as 4 pi times the ratio of the power per unit solid angle scattered in a specified direction of the power unit area in a plane wave incident on the scatter from a specified direction. Meanwhile, with the detection and stealth technology developing rapidly, the radar cross section (RCS) reduction has been a serious problem in military applications, and has attracted significant attentions recently [1]–[4]. Coating with radar absorbing materials (RAM), forming and using passive and active cancellation technology are normally methods in RCS reduction. And many new metamaterials are designed for RCS reduction. Such as electromagnetic band gap (EBG), Metamaterials absorber (MA), frequency selective surface (FSS) and so on [5]–[8]. However, most methods and metamaterials are limited to the narrowband RCS reduction.

Recently, some researchers have proposed the use of metamaterials in the design of Low-RCS reflectors and antennas. In [2], a broadband MA based on resistive high-impedance patch is used, and this structure is used in the microstrip slot antenna RCS reduction. The monostatic RCS is reduced in the wideband of 2-18 GHz. But no prototype is fabricated in this paper. In addition, FSS is usually used for out-band RCS reduction. Classical band-pass FSS radome or band-stop FSS reflector can meet the requirement of the transmissivity, beamwidth, and Low-RCS reflector [9], [10]. In recent years, the polarization rotation surfaces (PRS) has extensive applications in polarization control devices, circularly polarized antennas and RCS reduction. Literature [11] comprehensively considered the polarization conversion and polarization selection characteristics. A 90° transmission type polarization rotator in the THz band is designed. In [12], an ultra-thin 90° polarization rotator based on the optical rotation of chiral metamaterials is proposed. The highlight of this design is that the polarization rotation band can be changed within a certain range. A circularly polarized antenna is designed by PRS in [13]. It converts a linearly polarized wave into a circularly polarized wave. And the impedance bandwidth and gain characteristics of the antenna are greatly improved. However, these papers do not cover the issue of RCS reduction. Meanwhile, the narrowband PRS structure is

The associate editor coordinating the review of this manuscript and approving it for publication was Wanchen Yang.

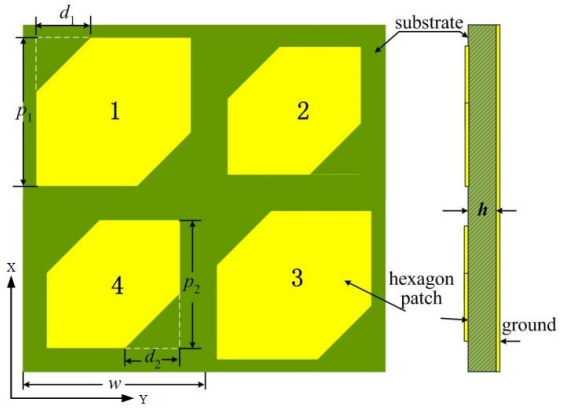

FIGURE 1. The configuration of the HPRS.

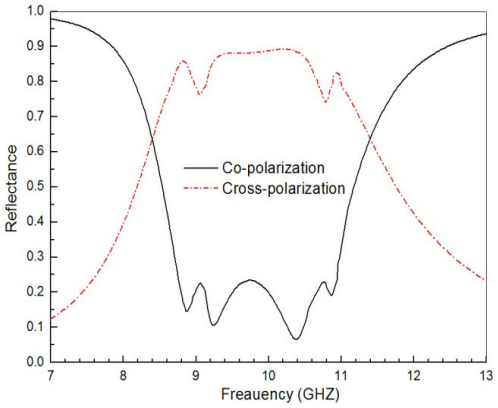

FIGURE 2. The simulated reflectance of the HPRS.

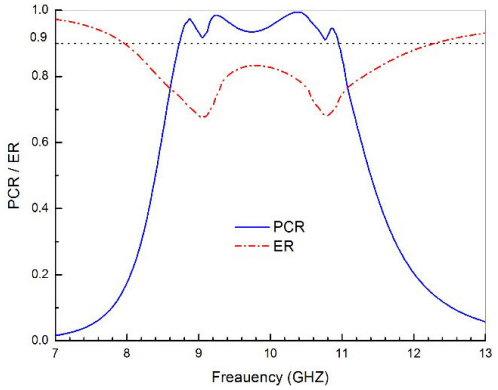

FIGURE 3. The simulated PCR and the ER of the HPRS.

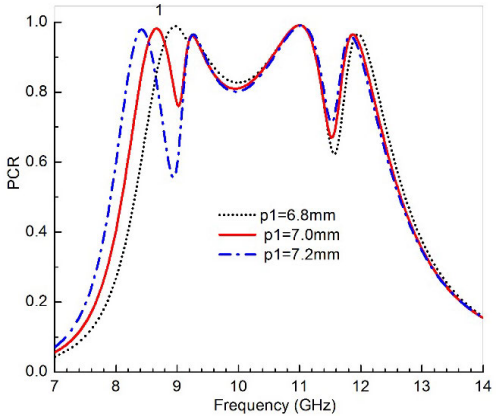

FIGURE 4. The simulated PCR of the HPRS for the case of different p1.

presented in the existing literature, which can only achieve narrowband RCS reduction [14]–[15].

Based on this, a wideband Hexagon Polarization Rotation Surfaces (HPRS) is introduced to achieve the wideband Low-RCS reflector. A 180°-phase difference is created by the PRS using chessboard-like geometry, which introduced 90° and −90° phase-shift, respectively. The scattering energy is redirected into off-normal directions by the HPRS, which enables the effective RCS reduction. The HPRS reflector can be used as a low-RCS reflector. Furthermore, the arrangement of the HPRS reflector has been changed. More RCS reduction is obtained by the improved arrangement [16]. The measured and simulated results show that the monostatic RCS of the HPRS has been considerably reduced. The monostatic RCS of the reflector can be reduced more than 20 dB by this method.

II. DESIGN OF THE HEXAGON POLARIZATION ROTATION SURFACES

The Hexagon Polarization Rotation Surfaces (HPRS) is composed of different sizes of hexagonal patch arrays, metal ground planes and dielectric substrate. The basic structure and parameters are shown in Figure 1. Copper conductors are used for both the patch and the ground plane with a thickness of 0.018 mm, and the electrical conductivity $\sigma = 5.8 \times 10^7$ S/m. The dielectric substrate is FR-4 with a relative dielectric constant of 4.4 and the loss tanδ of 0.02. In addition, the patch 1 and 3 are identical in size, and the size of the patch 2 and 4 are also the same, thereby corresponding to different resonance frequencies.

In order to broaden the bandwidth, a multi-point resonance method is used in this paper. The HPRS structure is combined with two sets of hexagonal patches of different sizes. The final parameters of the HPRS are: w=12 mm, p1=7.05 mm, p2=6.8 mm, d1=2.55 mm, d2=2.44 mm, h=1.6 mm. The simulated reflectance is shown in the Figure 2, and the PCR and the ER are shown in Figure 3. The PCR and the ER are defined as:

$$PCR = \frac{|\Gamma_{yx}|^2}{|\Gamma_{yx}|^2 + |\Gamma_{xx}|^2} \quad (1)$$

$$ER = |\Gamma_{yx}|^2 + |\Gamma_{xx}|^2 \quad (2)$$

In order to investigate how the parameters affect the reflection rotation characteristics of the HPRS, a series of parameter analysis are proposed. In Figure 4, p1 is increased from 6.8mm to 7.2mm with the other parameters fixed. It can be seen from Figure 4 that with the increase of p1, the resonant frequency of the peak 1 shifts to a lower frequency, while the remaining peaks are substantially unaffected. The parameter d1 has been investigated in Figure 5. As d1 increases, the resonant frequency of the peak 3 shifts to a higher frequency. And the d1 has little effect on other peaks.

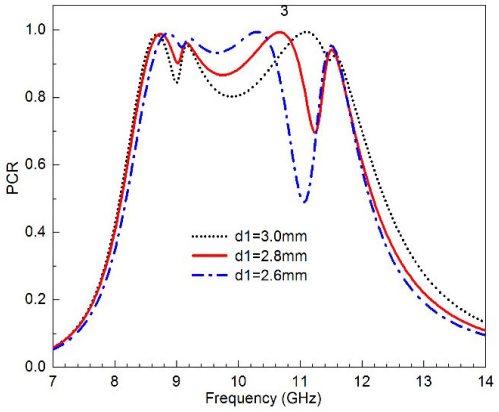

FIGURE 5. The simulated PCR of the HPRS for the case of different d1.

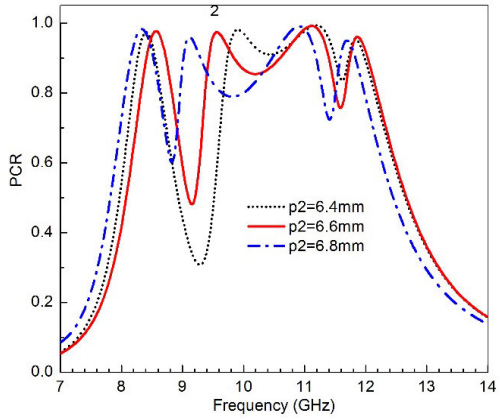

FIGURE 6. The simulated PCR of the HPRS for the case of different p2.

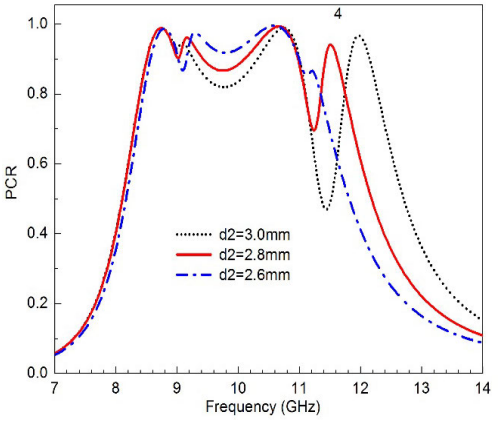

FIGURE 7. The simulated PCR of the HPRS for the case of different d2.

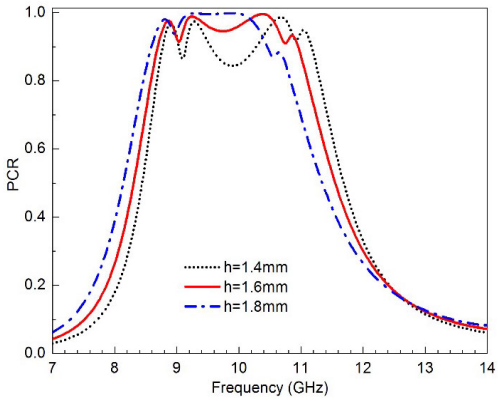

FIGURE 8. The simulated PCR of the HPRS for the case of different h.

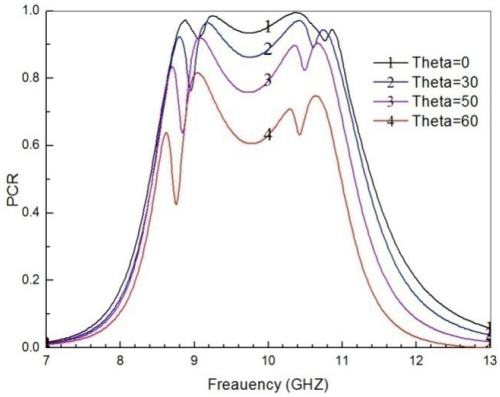

FIGURE 9. The simulated PCR of the HPRS under different incident angles.

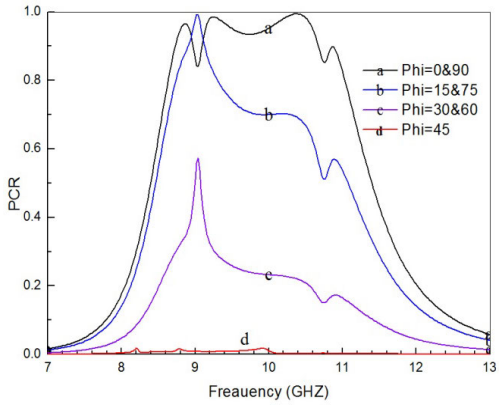

FIGURE 10. The simulated PCR of the HPRS under different polarization angles.

It can also be observed that the p1, d1 of the patches 1 and 3 can be used to regulate the resonant frequency of the peak 1 and 3. Similarly, it can be analyzed the p2 and d2 in Figure 6 and Figure 7. Figure 8 shows the effect of the thickness h of the dielectric substrate on PCR. When h is increased from 1.4 mm to 1.8 mm, peaks 3 and 4 are significantly shifted to a lower frequency.

Finally, the stability of the PRS under the oblique incident waves has been investigated. The effects of different incident angles θ and polarization angles φ are also analyzed. It can be seen from Figure 9, as the incident angle θ increases, the polarization conversion rate of the HPRS gradually decreases. However, the polarization conversion ratio is more than 60% in the frequency band of 8.48 GHz to 11.1 GHz when the incident angle increases to 50° It indicates that the proposed structure has a wide incident angle characteristic.

As shown in Figure 10, the PCR characteristic deteriorates sharply as the polarization angle φ changes. When the

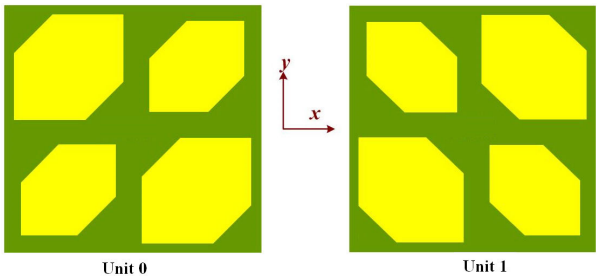

FIGURE 11. The Unit of the Low-RCS reflector.

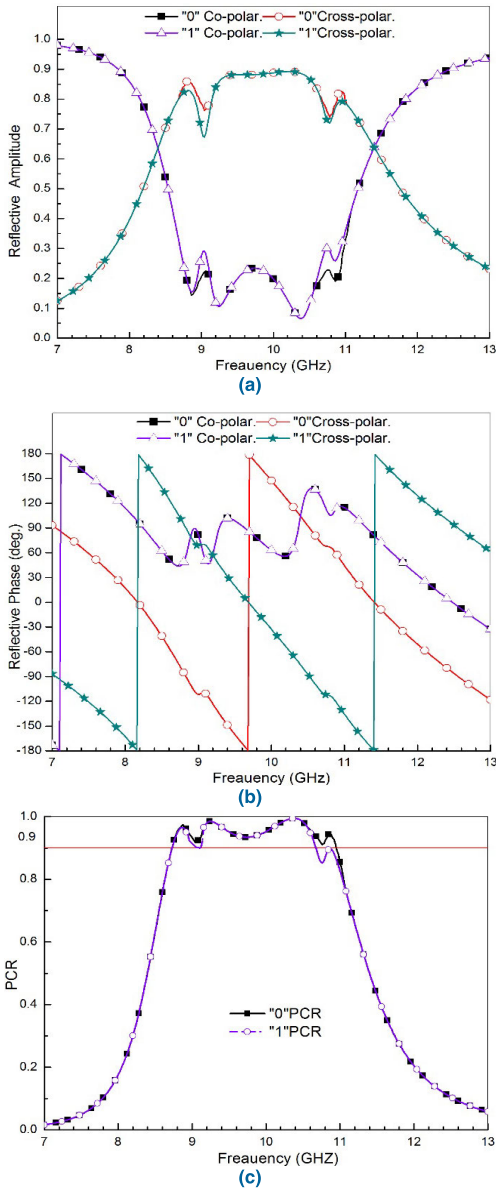

FIGURE 12. The simulated reflection coefficient of the HPRS. (a) amplitude, (b) phase, (c) PCR.

polarization angle increases, the polarization direction of the incident wave is changed. It is no longer a simple x-polarized wave or a y-polarized wave. Therefore, it no longer satisfies the conditions of polarization conversion.

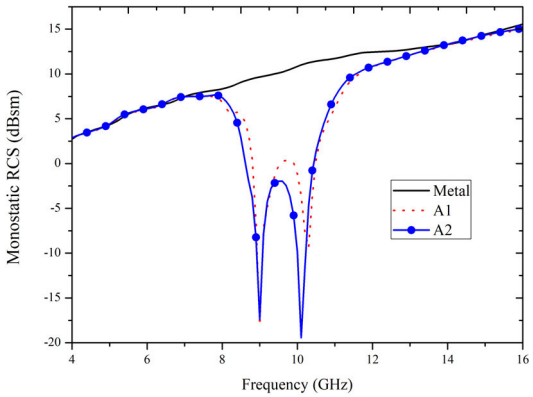

FIGURE 13. The comparison of the simulated monostatic RCS of the metal reflector, the A1 arrangement reflector and the A2 arrangement reflector.

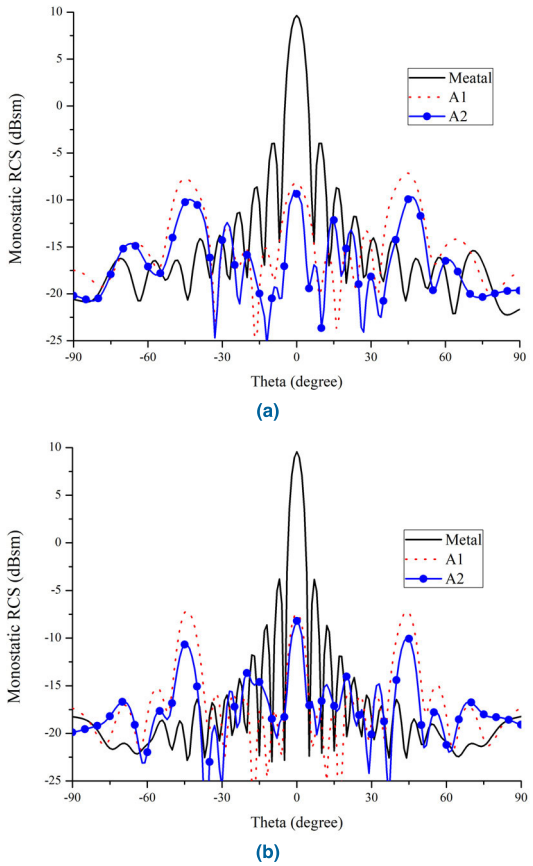

FIGURE 14. The comparison of the simulated RCS under different incident angles (9GHz). (a) xoz-plane, (b) yoz-plane.

III. LOW-RCS REFLECTOR BY THE HEXAGON POLARIZATION ROTATION SURFACES

As mentioned earlier, the RCS reduction is the most important technical approaches to implementing the stealth technology. It is well known that the metal plane has a strong scattering. In order to control the scattered waves, the destructive interference principle can be used to minimize the scattered field. In this paper, the destructive interference is enhanced by reasonably combining the unit "0" and "1". The scattering

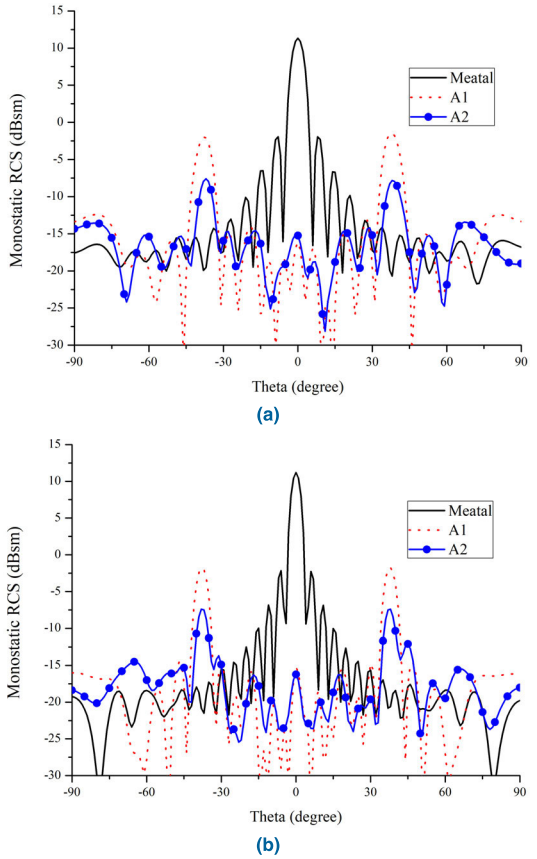

FIGURE 15. The comparison of the simulated RCS under different incident angles (10.2GHz). (a) xoz-plane, (b) yoz-plane.

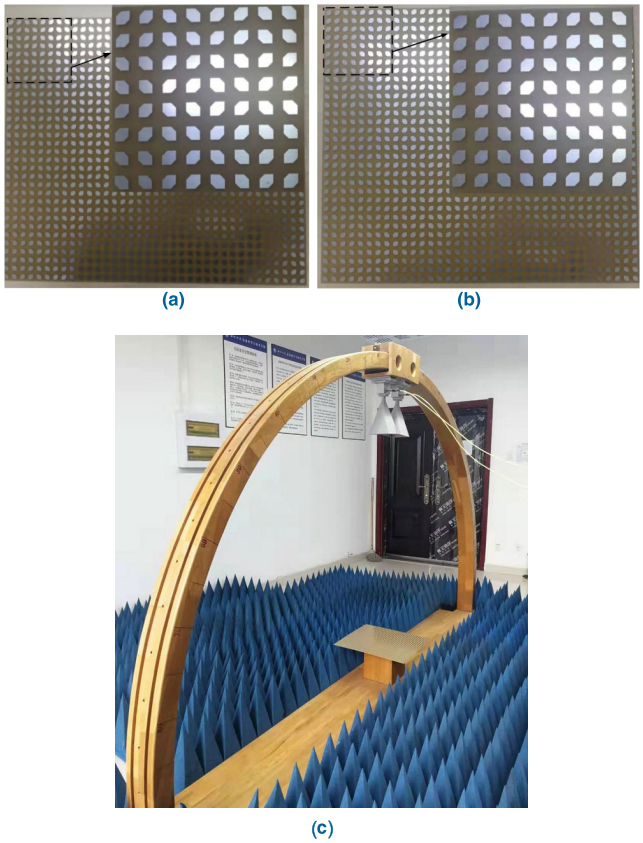

FIGURE 16. The photograph of the two reflectors. (a) A1, (b)A2, (c) measuring photo.

field distribution is effected, and the RCS of the reflector is reduced.

The HPRS unit can convert a linearly polarized wave into a reflected wave with 90° phase-shift in a wide band. In order to achieve a low-RCS reflector, the previous HPRS unit is known as unit "0"; then the HPRS unit is rotated by 90° and known as unit "1". The low-RCS reflector designed in this section is composed of "0" and "1" unit. Figure 11 shows the basic structure of the unit.

Assuming that x-polarized incident wave is illuminated, the reflection characteristics of each unit are simulated. Figure 12(a) and (b) show the amplitude and phase of the reflection coefficient of the unit "0" and "1", respectively. Figure 12 (c) shows the polarization conversion rate. The simulated results show that both forms of the units can achieve the 90° phase-shift, and the polarization conversion rate is greater than 90%.

However, A 180°-phase difference is created by the HPRS using different units, which introduced 90° and −90° phase-shift, respectively. The reflected waves are suppressed in some directions, and the low-RCS characteristic is achieved. Therefore, the above unit can be combined into a reflector by specific arrangement. In this paper, two arrangements are used. One is a uniform arrangement. The other is an optimized arrangement. The optimized matrix of [16] is used in this paper. The uniform arrangement is called A1 arrangement:

$$\begin{bmatrix} 1 & 0 & 1 & 0 & 1 & 0 & 1 & 0 \\ 0 & 1 & 0 & 1 & 0 & 1 & 0 & 1 \\ 1 & 0 & 1 & 0 & 1 & 0 & 1 & 0 \\ 0 & 1 & 0 & 1 & 0 & 1 & 0 & 1 \\ 1 & 0 & 1 & 0 & 1 & 0 & 1 & 0 \\ 0 & 1 & 0 & 1 & 0 & 1 & 0 & 1 \end{bmatrix} \tag{3}$$

The optimized arrangement is called A2 arrangement:

$$\begin{bmatrix} 1 & 0 & 1 & 0 & 1 & 1 & 1 & 0 \\ 0 & 1 & 0 & 1 & 0 & 1 & 0 & 1 \\ 0 & 1 & 0 & 1 & 1 & 0 & 1 & 0 \\ 1 & 0 & 0 & 1 & 0 & 0 & 0 & 1 \\ 0 & 1 & 0 & 0 & 1 & 1 & 0 & 1 \\ 1 & 1 & 1 & 1 & 0 & 0 & 0 & 0 \end{bmatrix} \tag{4}$$

The monostatic RCS of the metal reflector, the A1 arrangement reflector and the A2 arrangement reflector are evaluated. The incident wave is perpendicular to the reflector. Figure 13 shows the analysis of the monostatic RCS of these three reflectors. The incident wave is φ-polarization. As shown in Figure 13, there is RCS reduction of the reflector using HPRS during 8GHz -13GHz, and the largest reduction is more than 20 dB at 9GHz and 10.2 GHz. At the same time, it can be seen that the RCS reduction of the A2 arrangement

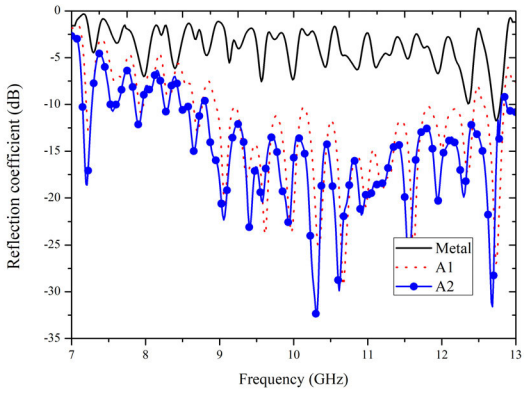

FIGURE 17. The comparison of the measured reflection coefficient.

reflector is more than the A1 arrangement reflector, especially at 9GHz and 10.2GHz. In order to compare the RCS reduction at 9GHz and 10.2GHz between A1 and A2 obviously, the comparison of the monostatic RCS under various angles of incident wave is analyzed.

The comparison of the monostatic RCS under various angles of incident wave is shown in Figure 14 and Figure 15, and the incident wave is φ-polarization. The frequency of the incident wave is 9GHz in Figure 14. Both the xoz-plane and the yoz-plane, RCS reduction of the two reflectors are achieved within the angles from $-35°$ to $+35°$. The monostatic RCS of the A2 arrangement reflector is slightly lower than A1. The frequency of the incident wave is 10.2GHz in Figure 15. Similar to previous results, the RCS reduction of the two reflectors are achieved within the angles from $-20°$ to $+20°$. The A2 arrangement reflector is also slightly better for RCS reduction.

Finally, the HPRS with A1 arrangement reflector and the A2 arrangement reflector are fabricated. In order to show the effect of this structure clearly. The previous A1 and A2 arrangement reflector are used as the array element of a 2×3 array. The photographs of the two reflectors are shown in Figure 16. The measured reflection coefficients (*xx*- polarization) of the two reflectors are obtained, as shown in Figure 17. It can be seen that the reflection coefficient of the two reflectors is significantly reduced in a wide band. The reflection coefficient of the A2 arrangement reflector is slightly lower than A1.

IV. CONCLUSION

A wideband Hexagon Polarization Rotation Surfaces (HPRS) is introduced to design a wideband Low-RCS reflector. The scattering energy is redirected into off-normal directions by the HPRS, which enables the effective RCS reduction. A uniform arrangement and an optimized arrangement are used in this paper. More RCS reduction is obtained by the optimized arrangement. The results show that the RCS of the HPRS has been considerably reduced. The monostatic RCS of the reflector can be reduced more than 20 dB by this method.

REFERENCES

[1] D. Pozar, "Radiation and scattering from a microstrip patch on a uniaxial substrate," *IEEE Trans. Antennas Propag.*, vol. 35, no. 6, pp. 613–621, Jun. 1987.
[2] S. Genovesi, F. Costa, and A. Monorchio, "Wideband radar cross section reduction of slot antennas arrays," *IEEE Trans. Antennas Propag.*, vol. 62, no. 1, pp. 163–173, Jan. 2014.
[3] F. Wang, K. Li, and Y. Ren, "Reconfigurable polarization rotation surfaces applied to the wideband antenna radar cross section reduction," *Int. J. RF Microw. Comput.-Aided Eng.*, vol. 28, no. 5, Jun. 2018, Art. no. e21262.
[4] T. Hong, Z. Zhao, W. Jiang, S. Xia, Y. Liu, and S. Gong, "Dual-band SIW cavity-backed slot array using TM_{020} and TM_{120} modes for 5G applications," *IEEE Trans. Antennas Propag.*, vol. 67, no. 5, pp. 3490–3495, May 2019.
[5] F. Wang, W. Jiang, T. Hong, H. Xue, S. Gong, and Y. Zhang, "Radar cross section reduction of wideband antenna with a novel wideband radar absorbing materials," *IET Microw. Antennas Propag.*, vol. 8, no. 7, pp. 491–497, May 2014.
[6] Y. Jia, Y. Liu, Y. J. Guo, K. Li, and S. Gong, "A dual-patch polarization rotation reflective surface and its application to ultra-wideband RCS reduction," *IEEE Trans. Antennas Propag.*, vol. 65, no. 6, pp. 3291–3295, Jun. 2017.
[7] S.-J. Li, J. Gao, X.-Y. Cao, Y. Zhao, Z. Zhang, and H.-X. Liu, "Loading metamaterial perfect absorber method for in-band radar cross section reduction based on the surface current distribution of array antennas," *IET Microw. Antenna Propag.*, vol. 9, no. 5, pp. 399–406, Apr. 2015.
[8] F. Wang, K. Li, and Y. Ren, "A novel reconfigurable FSS applied to the antenna radar cross section reduction," *Int. J. RF Microw. Comput.-Aided Eng.*, vol. 29, no. 7, Jul. 2019, Art. no. e21729.
[9] A. Edalati and K. Sarabandi, "Wideband, wide angle, polarization independent RCS reduction using nonabsorptive miniaturized-element frequency selective surfaces," *IEEE Trans. Antennas Propag.*, vol. 62, no. 2, pp. 747–754, Sep. 2014.
[10] S. R. Thummaluru, R. Kumar, and R. K. Chaudhary, "Isolation enhancement and radar cross section reduction of MIMO antenna with frequency selective surface," *IEEE Trans. Antennas Propag.*, vol. 66, no. 3, pp. 1595–1600, Mar. 2018.
[11] Y.-J. Chiang and T.-J. Yen, "A composite-metamaterial-based terahertz-wave polarization rotator with an ultrathin thickness, an excellent conversion ratio, and enhanced transmission," *Appl. Phys. Lett.*, vol. 102, Jan. 2013, Art. no. 011129.
[12] S. Kun, X. Zhao, Y. Liu, Q. Fu, and C. Luo, "A frequency-tunable 90°-polarization rotation device using composite chiral metamaterials," *Appl. Phys. Lett.*, vol. 103, Sep. 2013, Art. no. 101908.
[13] H. L. Zhu, S. W. Cheung, K. L. Chung, and T. I. Yuk, "Linear-to-circular polarization conversion using metasurface," *IEEE Trans. Antennas Propag.*, vol. 61, no. 9, pp. 4615–4623, Sep. 2013.
[14] Y. Liu, K. Li, Y. Jia, Y. Hao, S. Gong, and Y. J. Guo, "Wideband RCS reduction of a slot array antenna using polarization conversion metasurfaces," *IEEE Trans. Antennas Propag.*, vol. 64, no. 1, pp. 326–331, Jan. 2016.
[15] Y. Jia, Y. Liu, Y. J. Guo, K. Li, and S.-X. Gong, "Broadband polarization rotation reflective surfaces and their applications to RCS reduction," *IEEE Trans. Antennas Propag.*, vol. 64, no. 1, pp. 179–188, Jan. 2016.
[16] S. J. Li, X. Y. Cao, L. M. Xu, L. J. Zhou, H. H. Yang, J. F. Han, Z. Zhang, D. Zhang, X. Liu, C. Zhang, Y. J. Zheng, and Y. Zhao, "Ultra-broadband reflective metamaterial with rcs reduction based on polarization convertor, information entropy theory and genetic optimization algorithm," *Sci. Rep.*, vol. 6, Nov. 2016, Art. no. 37409.

ZHOU-HU DENG was born in Xi'an, Shannxi, China, in 1964. He received the B.Sc. degree in semiconductor physics and the M.Sc. degree in microelectronics engineering from Northwest University, China, in 1986 and 2006, respectively, where he is currently an Associate Professor with the School of Information Science and Technology.

His major research interest includes reliability design of electronic components, circuits, and antenna.

FU-WEI WANG was born in Xi'an, Shannxi, China, in 1987. He received the B.S. degree in electronic information engineering and the Ph.D. degree in electromagnetic wave and microwave technology from Xidian University, Xi'an, China, in 2009 and 2014, respectively.

He is currently a Lecturer with the School of Information Science and Technology, Northwest University, Xi'an. His research interests include antenna scattering, antenna RCS reduction, and metamaterials.

YU-HUI REN received the B.S. degree in communication engineering from the China University of Geosciences, Wuhan, China, in 2003, the M.S. degree in signal and information processing from Northwest University, Xi'an, China, in 2010, and the Ph.D. degree in electromagnetic wave and microwave technology from Northwestern Polytechnical University, Xi'an, in 2017.

He is currently an Associate Professor with the School of Information Science and Technology, Northwest University. He has authored or coauthored over ten articles in the SCI journals. His research interests include antenna array designs, metamaterials, and UWB antenna.

KE LI received the B.S. degree in electronic information engineering and the Ph.D. degree in electromagnetic wave and microwave technology from Xidian University, Xi'an, China, in 2011 and 2016, respectively.

She is currently a Lecturer with the School of Information Science and Technology, Northwest University, Xi'an. Her research interests include multiband antenna design, reconfigurable antennas, and metamaterials.

BAO-JIAN GAO was born in Baoji, Shaanxi, China, in 1963. He received the B.S. degree in mathematics from the Northwest University, Xi'an, in 1985, and the M.S. degree in electronic and communications systems from Xidian University, Xi'an, in 1988.

From 1988 to 2001, he was a Senior Engineer with the Telemeter and Telecontrol Laboratory, Xi'an Electromechanical Institute. Since 2001, he has been an Associate Professor with Northwest University. He is the author of one book and more than 64 articles. His research interests include physical layer security, antenna design, and microwave circuit.